J. Cent. South Univ. (2015) 22: 880−886
DOI: 10.1007/s11771-015-2597-4

Springer

Formation of passivation film during pyrrhotite bioleached by pure *L. ferriphilum* and mixed culture of *L. ferriphilum* and *A. caldus*

GU Guo-hua(顾帼华)[1], YANG Hui-sha(杨慧沙)[1], HU Ke-ting(胡可婷)[1],
WANG Chong-qing(王重庆)[2], XIONG Xian-xue(熊先学)[1], LI Shuang-ke(李双棵)[1]

1. School of Mineral Processing and Bioengineering, Central South University, Changsha 410083, China;
2. School of Chemistry and Chemical Engineering, Central South University, Changsha 410083, China

Abstract: Bioleaching and electrochemical experiments were conducted to evaluate pyrrhotite dissolution in the presence of pure *L. ferriphilum* and mixed culture of *L. ferriphilum* and *A. caldus*. The results indicate that the pyrrhotite oxidation behavior is the preferential dissolution of iron accompanied with the massive formation of sulfur in the presence of *L. ferriphilum*, which significantly hinders the leaching efficiency. Comparatively, the leaching rate of pyrrhotite distinctly increases by 68% in the mixed culture of *L. ferriphilum* and *A. caldus* at the 3rd day. But, the accumulated ferric ions and high pH value produced by bioleaching process can give rise to the rapid formation of jarosite, which is the primary passivation film blocking continuous iron extraction during bioleaching by the mixed culture. The addition of *A. caldus* during leaching by *L. ferriphilum* can accelerate the oxidation rate of pyrrhotite, but not change the electrochemical oxidation mechanisms of pyrrhotite. XRD and SEM/EDS analyses as well as electrochemical study confirm the above conclusions.

Key words: pyrrhotite; passivation film; bioleaching; moderately thermophilic microorganisms; electrochemistry

1 Introduction

Pyrrhotite ($Fe_{1-x}S$) is one of the most common and abundant sulfide minerals presented in mining wastes from the processing of base-metals or precious metal ores [1−2]. The exposure of pyrrhotite to the environment results in release of weathering products containing acid due to the oxidation and hydrolysis reactions in soil and geological materials under earth surface conditions [3−5]. Recently, the technique of iron bioleaching has been developed due to its advantages such as short flows, simple operation, low investment and friendly environment [6−8]. However, the bottlenecks of bioleaching, such as low leaching rate and efficiency, limit its development [9−10], because the insoluble passivation layer on the surface of the pyrrhotite significantly hinders the leaching efficiency [11−12].

STEGER [13] and SANTOS et al [14] reported that the predominant oxidation products of pyrrhotite were elemental sulfur (Eqs. (1) and (2)). BUCKLEY et al [15] studied the pyrrhotite dissolution at pH 4.6, 9.2, and 13.0 employing cyclic voltammetry, and the results demonstrated that elemental sulfur was the main product of the mineral oxidation and sulfate yield depended on pH. There are also a great number of surface analytical investigations of pyrrhotite [16−18], many of which related to the nature of the reactions occurring at the interface between pyrrhotite and air or water during weathering. However, there is no depth study on the factors blocking the reactivity of pyrrhotite in the presence of bacteria by application of electrochemical and spectroscopic techniques.

In this work, the formations of passive film during pyrrhotite bioleaching by pure *L. ferriphilum* and mixed culture of *L. ferriphilum* and *A. caldus* were studied in detail. The investigation on bioleaching efficiency and the change of products elaborates the reason of pyrrhotite passivation and offers some insights into the mechanism of pyrrhotite bioleaching. Electrochemical technique was also applied to investigating the initial oxidation and passivation of pyrrhotite.

$$Fe_{1-x}S + 0.5O_2 + 2H^+ \rightarrow (1-3x)Fe^{2+} + 2xFe^{3+} + S^0 + H_2O \quad (1)$$

$$Fe_{1-x}S + (2-2x)Fe^{3+} \rightarrow (3-3x)Fe^{2+} + S^0 \quad (2)$$

Foundation item: Project(2010CB630903) supported by the National Basic Research Program of China; Project(51374249) supported by the National Natural Science Foundation of China
Received date: 2013−12−23; **Accepted date:** 2014−03−18
Corresponding author: GU Guo-hua, Professor; Tel: +86−13975151469; E-mail: guguohua@126.com

2 Experimental

2.1 Pyrrhotite preparation

The samples of pyrrhotite used in the bioleaching tests were from Dabaoshan in Guangdong Province, China. The samples were splintered into small fragments and dry ground in a porcelain ball milling, and then were sieved to obtain suitable size less than 0.074 mm for bioleaching experiments. Chemical analyses showed that the pure pyrrhotite contained 58.28%Fe, 37.7%S (mass fraction) and there was also a small amount of quartz in it.

The electrodes of pyrrhotite used in this work were prepared from high-purity pyrrhotite samples. To fit specially designed electrode sets and expose only one side, all electrodes were cut into about *d*12 mm×5 mm cylinders. The effective area of pyrrhotite electrode was 0.75 cm^2.

2.2 Microorganisms and culture media

L. ferriphilum (DQ343299) and *A. caldus* (DQ256484) used in the experiments were provided by the Key Laboratory of Biometallurgy in Central South University, China. They were grown in medium using rotary shakers at 160 r/min with the initial pH 1.6 and 2.0 and the temperatures of 40 °C and 45 °C, respectively. The medium consisted of $(NH_4)_2SO_4$ 3.0 g/L, KCl 0.1 g/L, K_2HPO_4 0.5 g/L, $MgSO_4·7H_2O$ 0.5 g/L and $Ca(NO_3)_2$ 0.01 g/L. $FeSO_4·7H_2O$ 44.7 g/L and S 10 g/L were added separately to support the growth of *L. ferriphilum* and *A. caldus*. When the bacteria reached the logarithmic growth period, cells were harvested by centrifugation and washed three times with distilled water.

2.3 Bioleaching tests

Bioleaching tests were carried out in 250 mL Erlenmeyer flasks containing 100 mL medium at initial pH 1.6 and 40 °C. The flasks were placed in a rotary shaker at 160 r/min. The mineral concentration was 1% (w/v) and the inoculation was $5×10^7$ cell/mL. The parallel experiment without cells, but with the same culture medium and pyrrhotite, was run as abiotic control. The solution pH was adjusted periodically to the target pH value with diluted sulfuric acid.

Periodically, water evaporation was restored; pH and redox potential were recorded; a 3 mL sample was removed from the liquid to obtain the levels of Fe^{2+} and total iron in solution. The redox potentials were measured using a platinum electrode combined with an $Hg/HgCl_2$ reference electrode. The concentration of ferrous ion in the solution was determined by titration with potassium dichromate ($K_2Cr_2O_7$). Ferric iron concentration is the concentration of total iron minus the concentration of ferrous irons. The pH value in the leaching solution was measured with a pH-meter (SJ−4A).

2.4 XRD and SEM/EDS analyses

The leaching residues were filtered and air dried for XRD and SEM/EDS analyses. XRD tests were conducted using an X-ray diffractometer (Model D/Max2500PC) with Cu K_α radiation (λ=1.54056 Å) in the range of 2θ from 5° to 80°. A scanning electron microscope (JSM−6360LV) equipped with an EDS was used to determine the pyrrhotite surface changes during bioleaching.

2.5 Electrochemical study

The electrochemical measurements were performed using a three-electrode system with the following three electrodes: the working electrode (pyrrhotite), the counter electrode (graphite) and the reference electrode (Ag/AgCl). The electrochemical experiments were carried out in electrolyte solution, consisting of $(NH_4)_2SO_4$ 3.0 g/L, KCl 0.1 g/L, K_2HPO_4 0.5 g/L, $MgSO_4·7H_2O$ 0.5 g/L and $Ca(NO_3)_2$ 0.01 g/L. Before each electrochemical test, the electrode was polished by $1000^{\#}$ silicon carbide paper in order to keep the working face being clean, smooth and fresh.

3 Results and discussion

3.1 Bioleaching experiments

Comparisons of pyrrhotite leached by pure *L. ferriphilum* and mixed culture of *L. ferriphilum* and *A. caldus* are shown in Fig. 1. In the case of mixed culture of *L. ferriphilum* and *A. caldus*, the total iron extraction reaches 85.68% just at the 3rd day, and thereafter the leaching rate begins to decline and the total iron extraction is descended to 58.65% at the 9th day. Comparatively, the leaching process is strongly restricted in the pure culture of *L. ferriphilum*: the total iron extraction is only 31.11% at the end of leaching, which is a little higher than that in abiotic control. The results imply that the addition of sulfur oxidizing bacteria significantly increases the leaching rate of pyrrhotite.

Figure 1(b) demonstrates that ferric ion extraction in mixed culture rises rapidly from the beginning to the 3rd day, at which the ferric mass concentration in solution is 3.99 g/L. And then, it reduces to 1.73 g/L at the 9th day, confirming that the ferric ions have been consumed due to ferric ion reduction via pyrrhotite oxidation (Eq. (2)) or the precipitation of the soluble ferric ions as jarosite (Eq. (3)). Interestingly, the leaching rate of ferric ion for the exposure to *L. ferriphilum* medium almost stays around zero during the leaching period, and it is

noticeable that the bioleaching efficiency has a close connection with the ferric ion concentration. It is generally accepted that ferric ions as oxidants are effective for leaching pyrrhotite [19]. Therefore, the leaching process is inhibited when the concentration of ferric ion in solution is low.

$$K^{+}+3Fe^{3+}+2SO_4^{2-}+6H_2O \rightarrow KFe_3(SO_4)_2(OH)_6+6H^{+} \quad (3)$$

Referring to the redox potential curves, it is found that the changed trend of redox potential is very similar to that of ferric ion concentration after leaching for one day, for redox potential is corresponding to the Fe^{3+}-to-Fe^{2+} mole ratio. The results show that the redox potential in the presence of mixed culture initially decreases from 399 mV (vs. SCE) to 325 mV (vs. SCE) after leaching for one day. It is because iron preferentially dissolved from pyrrhotite (Eq. (1)), which results in the increase of the Fe^{2+}/Fe^{3+} ratio. The redox potential, afterwards, rises sharply to 642 mV (vs. SCE) after leaching for 5 d, and it declines slightly in the end. However, the value of the redox potential at the 9th day is not less than 580 mV (vs. SCE) due to the consumption of ferric ions. As anticipates, the redox potential in pure culture of *L. ferriphilum* reaches a plateau around 220 mV (vs. SCE) after one day, which is close to that in abiotic system.

The solution pH was adjusted periodically to the target pH value with diluted sulfuric acid. Figure 1(d) indicates that the pH value in mixed culture changes dramatically from the beginning to the 3rd day. This could be explained by the protonic attack during acidic dissolution of pyrrhotite (Eqs. (1) and (4)). Later on, pH tends to decline from the 4th day to the 9th day, and finally decreases to 1.22, demonstrating that the oxidation of elemental sulfur (Eq. (5)) and the formation of jarosite (Eq. (3)) exceed the oxidation of pyrrhotite. In the case of the pure culture of *L. ferriphilum* and abiotic control, the changed trend of pH value is slightly obvious in the first 3 d, and then increases slowly until the end of leaching. The results imply that extending leaching time results in a gradual passivation of pyrrhotite where iron dissolution leveled off.

$$2Fe^{2+}+0.5O_2+2H^{+} \xrightarrow{\text{Bacteria}} 2Fe^{3+}+H_2O \quad (4)$$

$$S+3/2O_2+H_2O \xrightarrow{\text{Bacteria}} H_2SO_4 \quad (5)$$

3.2 XRD and SEM/EDS analyses of bioleaching residues

In order to examine the role of passivation film of pyrrhotite during bioleaching by pure *L. ferriphilum* and mixed culture of *L. ferriphilum* and *A. caldus*, XRD and SEM/EDS analyses of bioleaching residues were conducted. Figure 2(a) shows that the residues leached

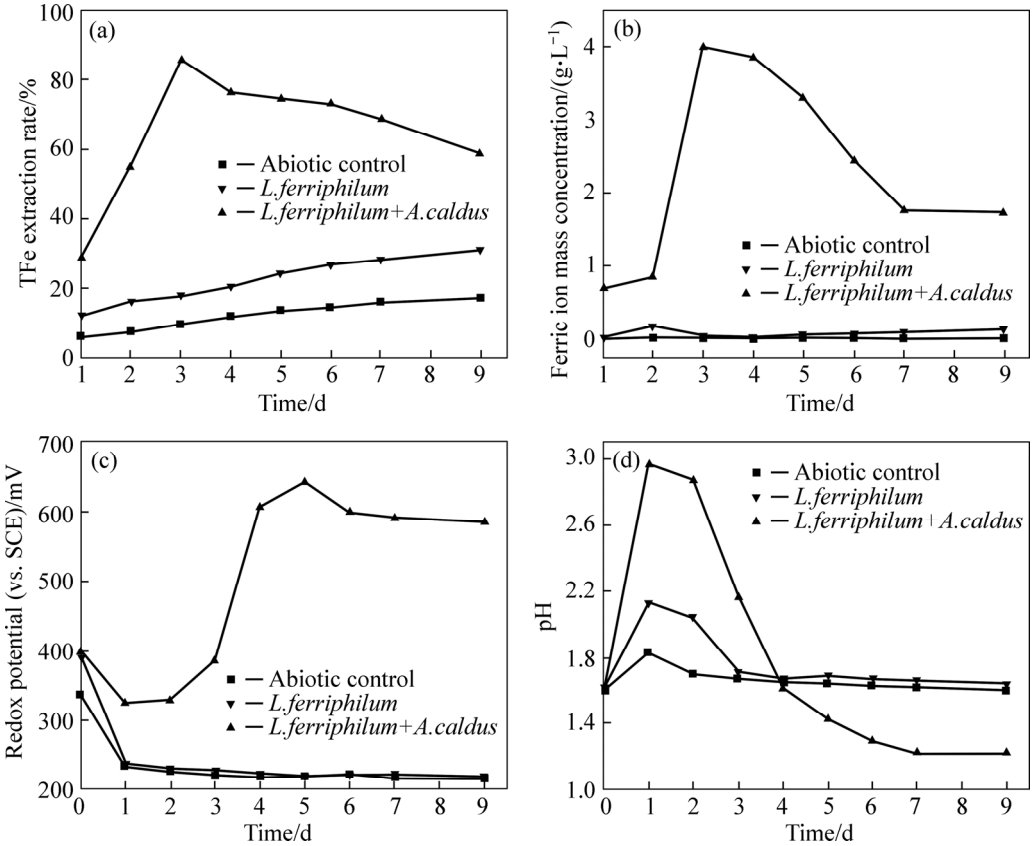

Fig. 1 Total iron extraction rate (a), ferric ion concentration (b), redox potential (c) and pH value (d) changes during bioleaching of pyrrhotite at pH 1.6 and 40 °C

for different leaching time in abiotic control consist mainly of pyrrhotite and sulfur. It indicates that sulfur is the predominant oxidation product of pyrrhotite under acidic leaching condition.

Figure 2(b) presents the XRD patterns of the residues after leaching for 3, 6, 9 d in the pure culture of *L. ferriphilum*. The XRD pattern of the residue leached for 3 d shows peaks corresponding to sulfur, confirming the formation of passivation film of pyrrhotite at the initial of pyrrhotite bioleaching (Eqs. (1) and (2)). As bioleaching process continues, no peaks corresponding to new product appear after 6 or 9 d of bioleaching.

From Fig. 2(c), it can be observed that the main compositions of the residues are pyrrhotite, sulfur (Eqs. (1) and (2)) and jarosite (Eq. (3)) after leaching for 3 d in the mixed culture of *L. ferriphilum* and *A. caldus*. Thus, it is obvious that jarosite is prone to be generated within a short time during pyrrhotite bioleaching by mixed culture. After leaching for 6 d, the main compositions of the residue are sulfur and jarosite. Furthermore, pyrrhotite is not detected in the residues because of the cover of sulfur and jarosite. The XRD results show that the composition after 9 d remains the same as that after 6 d; nonetheless, peaks of sulfur are weakened. It indicates that sulfur is gradually oxidized by *A. caldus* at the end of bioleaching (Eq. (5)), and jarosite is the primary passivation film blocking continuous iron extraction in the later stage of bioleaching process.

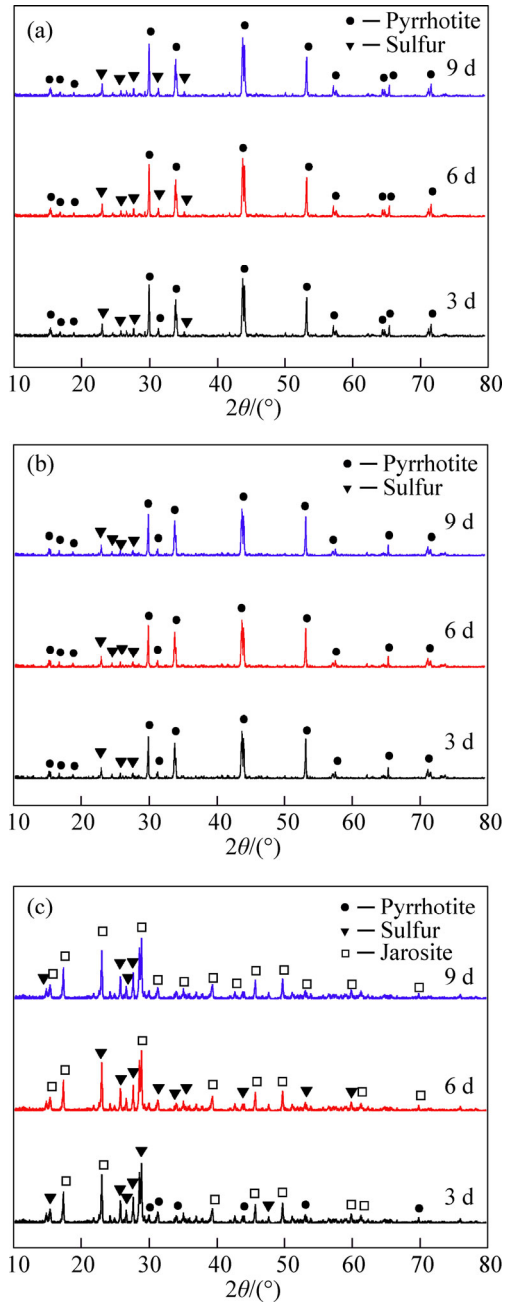

Fig. 2 XRD patterns of pyrrhotite residues leached for 3, 6 and 9 d under different leaching conditions: (a) Abiotic control; (b) *L. ferriphilum*; (c) *L. ferriphilum* and *A. caldus*

Scanning electron micrographs of the pyrrhotite surface leached in abiotic control for 3, 6, 9 d are shown in Figs. 3 ((a_1), (a_2), and (a_3)). It can be found that the pyrrhotite surface has no significant difference after different leaching time. The surface exhibits insignificant dissolution features, since it is relatively smooth and there are few deposits on it.

The surface morphology exposed to *L. ferriphilum* is obviously different from that in abiotic control. From Figs. 3 ((b_2) and (b_3)), numerous of leaching products are adsorbed on the mineral surface. In addition, the EDS analysis of the residues leached by *L. ferriphilum* for 3 d listed in Table 1 shows that the mass fractions of Fe and S were 65.38% and 33.61%, respectively. After bioleaching for 9 d, the mass fraction of Fe falls to 56.12%, and conversely, the mass fraction of S rises to 42.79%. The results indicate that the surface sulfur element is relatively rich after bioleaching of pyrrhotite. It can be seen in Fig. 2(b) that only sulfur is the product generated after 9 d of bioleaching. Hence, it further illustrates that the formation of elemental sulfur is the main factor hindering the leaching effect of pyrrhotite bioleached by *L. ferriphilum*.

The morphologies of pyrrhotite residues leached by mixed culture of *L. ferriphilum* and *A. caldus* for 3, 6, 9 d are shown in Figs. 3 ((c_1), (c_2), and (c_3)). Obviously, sulfur and jarosite identified by XRD analysis as shown in Fig. 2(c) have coated on the pyrrhotite surface after bioleaching for 3 d. Subsequently, the dense reaction products (sulfur and jarosite) after being bioleached for 6 d almost wrap pyrrhotite all up. After 9 d, a considerable amount of precipitates containing jarosite and sulfur are still on pyrrhotite surface. Also, the shape and morphology of the particles are similar corresponding with jarosite. Furthermore, the EDS analysis listed in Table 2 indicates that S compound is enriched on the surface of pyrrhotite after 3 d, which implies that the dominating passivation film is sulfur in

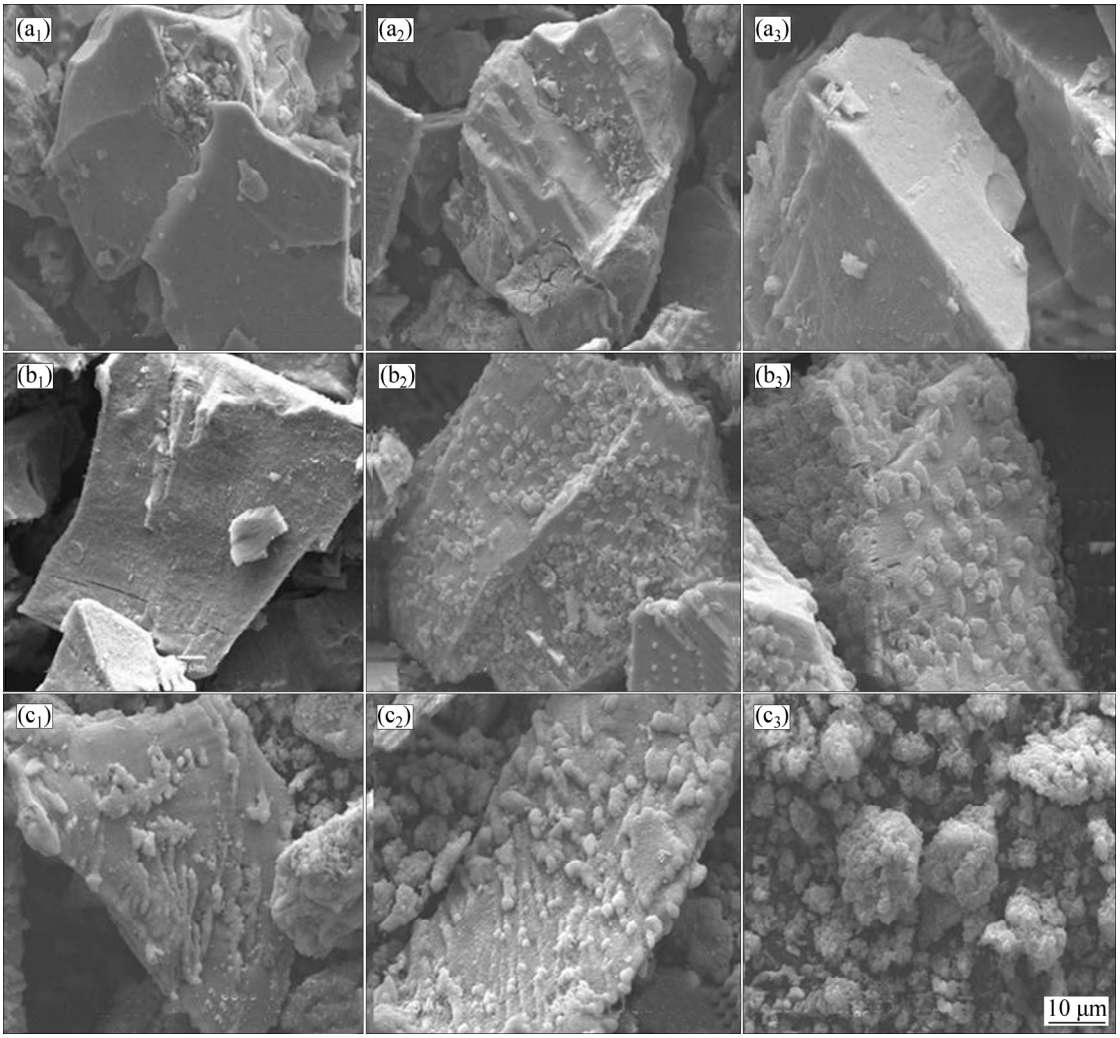

Fig. 3 SEM images of pyrrhotite residues leached under different conditions: (a_1) Abiotic control for 3 d; (a_2) Abiotic control for 6 d; (a_3) Abiotic control for 9 d; (b_1) *L. ferriphilum* for 3 d; (b_2) *L. ferriphilum* for 6 d; (b_3) *L. ferriphilum* for 9 d; (c_1) *L. ferriphilum* and *A. caldus* for 3 d; (c_2) *L. ferriphilum* and *A. caldus* for 6 d; (c_3) *L. ferriphilum* and *A. caldus* for 9 d

Table 1 Results of EDS microanalysis for pyrrhotite residues leached by pure culture of *L. ferriphilum* at different leaching time

Time/d	*w*/%			*x*%		
	S	Fe	O	S	Fe	O
3	33.61	65.38	0.5	46.22	51.61	1.37
6	40.49	58.44	1.06	53.27	43.94	2.8
9	42.79	56.12	1.09	55.42	41.74	2.84

Table 2 Results of EDS microanalysis for pyrrhotite residues leached by mixed culture of *L. ferriphilum* and *A. caldus* at different leaching time

Time/	*w*%				*x*/%			
d	S	Fe	O	K	S	Fe	O	K
3	56.23	36.00	4.53	3.23	63.54	23.24	10.24	2.99
6	49.56	40.28	5.70	4.45	56.5	26.24	13.00	4.16
9	24.84	59.16	6.12	9.87	31.45	42.80	15.50	10.25

the initial stage. However, as the leaching time is extended, Fe compound is enriched and jarosite is the primary passivation film instead of sulfur, which blocks continuous iron extraction in the presence of mixed culture of *L. ferriphilum* and *A. caldus*.

3.3 Electrochemical analysis

As mentioned in the materials and methods section, the electrodes were stabilized in the electrolyte for 20 min before starting each electrochemical test. Figure 4 shows the cyclic voltammograms obtained from the pyrrhotite electrode in the presence of pure *L. ferriphilum* and mixed culture of *L. ferriphilum* and *A. caldus*. Cycles were performed from −500 mV (vs. SHE) to 1200 mV (vs. SHE), then to −500 mV (vs. SHE). All cyclic voltammograms were carried out at a scan rate of 20 mV/s.

The curve obtained is similar to that obtained by ALMEIDA and GIANNETTI [18]. Three anodic peaks

(A1, A2 and A3) and three cathodic peaks (C1, C2 and C3) are detected in the *L. ferriphilum* medium. The anodic peak A1 is attributed to the formation of elemental sulfur [18] (Eq. (6)). During this step, as ferrous ions go to the solution, the accumulation of sulfur on the electrode surface is expected to occur. This accumulation could be interpreted by the formation of elemental sulfur layer [18]. It is evident that peak A2 appears at 600−800 mV (vs. SHE), and BIEGLER and HORNE [20] and NAVA et al [21] attributed this peak to the oxidation of Fe^{2+} to Fe^{3+} (Eq. (7)). When potential continues forward scanning, anode oxidation peak A3 is found at around 1000 mV (vs. SHE), which represents the oxidation of sulfur to sulphuric acid [21], based on the reaction of Eq. (8).

In the inverse scan, there is a series of reduction peaks between 600 mV (vs.SHE) and −400 mV (vs.SHE). Peak C1 has usually been assigned to the reduction of ferric ions [22−23] (Eq. (9)). The sulfur/intermediate possibly reduces in peak C2, acting as a precursor for the formation of elemental sulfur [15]. A tiny cathodic peak C3 at about −300 mV (vs. SHE) is observed, which is assigned to the reduction of elemental sulfur to H_2S [15] (Eq. (10)).

$$Fe_{1-x}S \rightarrow (1-x)Fe^{2+} + S^0 + 2(1-x)e \quad (6)$$

$$Fe^{2+} \rightarrow Fe^{3+} + e \quad (7)$$

$$S + 4H_2O \rightarrow SO_4^{2-} + 8H^+ + 6e \quad (8)$$

$$Fe^{3+} + e \rightarrow Fe^{2+} \quad (9)$$

$$S + 2H^+ + 2e \rightarrow H_2S \quad (10)$$

By comparison, Fig. 4 also shows that the anodic peaks and cathodic peaks of pyrrhotite have no significant difference with or without involvement of *A. caldus*. It can be illustrated that the mechanisms of pyrrhotite oxidation are identical in the culture with different types of bacteria. But the current density of peaks A2′ and A3′ are obviously higher when *A. caldus* is added in the presence of *L. ferriphilum*, verifying that *A. caldus* can effectively eliminate the elemental sulfur layer covered on the pyrrhotite electrode, which is beneficial to the pyrrhotite bioleaching. In addition, the results also confirmed that sulfur is the main product of pyrrhotite oxidation.

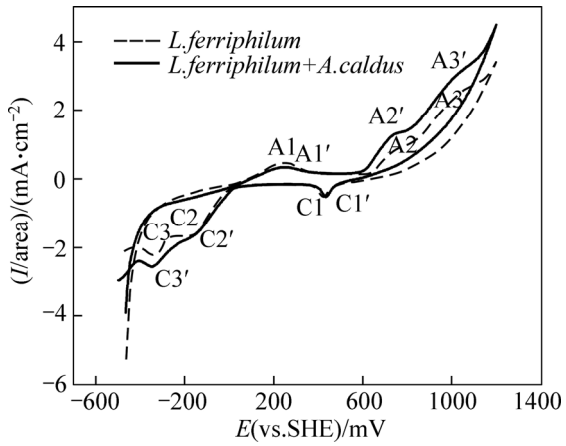

Fig. 4 Cyclic voltammetry curves of pyrrhotite electrode in medium with pure and mixed culture of *L. ferriphilum* and *A. caldus* at pH 1.6 and 40 °C

4 Conclusions

1) The low iron extraction rate in the presence of *L. ferriphilum* is due to the elemental sulfur layer covering on pyrrhotite surface.

2) The elemental sulfur layer can inhibit the diffusion of reactants (such as Fe^{3+} and bacteria) to the pyrrhotite surface.

3) *A. caldus* can effectively eliminate the passivation layer, but high rate of pyrrhotite oxidation results in the accumulation of ferric ions and high pH value and thus accelerates the rapid formation of jarosite at the early stage of pyrrhotite bioleaching process.

4) Jarosite is the primary passivation film hindering iron extraction during pyrrhotite bioleached by mixed culture of *L. ferriphilum* and *A. caldus*.

References

[1] ZHAO Kai-le, GU Guo-hua, LI Shuang-ke. Electrochemistry of oxidation of pyrrhotite in presence and absence of *Acidthiobacillus ferrooxidans* [J]. Journal of Central South University: Science and Technology, 2011, 42(10): 2887−2892. (in Chinese)

[2] GU Guo-hua, ZHAO Kai-le, QIU Guan-zhao, HU Yu-hua, SUN Xiao-jun. Effects of *Leptospirillum ferriphilum* and *Acidithiobacillus caldus* on surface properties of pyrrhotite [J]. Hydrometallurgy, 2009, 100(1/2): 72−75.

[3] WANG Hong-mei, BIGHAM J Y, TUOVINEN O H. Oxidation of marcasite and pyrite by iron-oxidizing bacteria and archaea [J]. Hydrometallurgy, 2007, 88(1/2/3/4): 127−131.

[4] LIU Yun, DANG Zhi, LU Gui-ning, WU Ping-xiao, FENG Chun-hua, YI Xiao-yun. Utilization of electrochemical impedance spectroscopy for monitoring pyrite oxidation in the presence and absence of *Acidithiobacillus ferrooxidans* [J]. Minerals Engineering, 2011, 24(8): 833−838.

[5] GLEISNER M, HERBERT R. Pyrite oxidation by *Acidithiobacillus ferrooxidans* at various concentrations of dissolved oxygen [J]. Chemical Geology, 2006, 225(1/2): 16−29.

[6] YANG Hong-ying, YANG Li. Bacterial metallurgy [M]. Beijing: Chemical Industry Press, 2006: 10−18. (in Chinese)

[7] SMITH R W, MISRA M, DUBEL J. Mineral bioprocessing and the future [J]. Minerals Engineering, 1991, 4(7/8/9/10/11): 1127−1141.

[8] PAN Hao-dan, YANG Hong-ying, TONG Lin-lin, ZHONG Cong-bin, ZHAO Yu-shan. Control method of chalcopyrite passivation in bioleaching [J]. Transactions of Nonferrous Metals Society of China, 2012, 22(9): 2256−2260.

[9] STOTT M B, WATLING H R, FRANZMANN P D, SUTTON D. The role of iron-hydroxy precipitates in the passivation of chalcopyrite during bioleaching [J]. Minerals Engineering, 2000,

13(10): 1117−1127.

[10] DEVECI H, AKCIL A, ALP I. Bioleaching of complex zinc sulphide using mesophilic and thermophilic bacteria: Comparative importance of pH and iron [J]. Hydrometallurgy, 2004, 73(3/4): 293−303.

[11] PAN Hao-dan, YANG Hong-ying, CHEN Shi-dong, LI Wei-tao. Study of passivation phenomenon on chalcopyrite surface under different conditions [C]// Memoir of the 8th Annual Conference of Transactions of Nonferrous Metals Society of China. Beijing: The Nonferrous Metals Society of China, 2010: 146−151. (in Chinese)

[12] YANG Hong-ying, PAN Hao-dan, TONG Lin-lin, LIU Yuan-yuan. Formation process of biological oxide film on chalcopyrite crystal surface [J]. Acta Metallurgica Sinica, 2012, 48(9): 1145−1152. (in Chinese)

[13] STEGER H F. Oxidation of sulfide minerals: VII. Effect of temperature and relative humidity on the oxidation of pyrrhotite [J]. Chemical Geology, 1982, 35: 281−295.

[14] SANTOS L R G, BARBOSA A F, SOUZA A D. Bioleaching of a complex nickel-iron concentrate by mesophile bacteria [J]. Minerals Engineering, 2006, 19(12): 1251−1258.

[15] BUCKLEY A N, HAMILTON I C, WOODS R. Studies of the surface oxidation of pyrite and pyrrhotite using X-ray photoelectron spectroscopy and linear potential sweep voltammetry [J]. The Electrochemical Society, 1988, 88: 234−246.

[16] BUCKLEY A N, WOODS R. X-ray photoelectron spectroscopy of oxidized pyrrhotite surfaces: I. Exposure to air [J]. Appl Surf Sci, 1985, 22: 280−287.

[17] BUCKLEY A N, WOODS R. X-ray photoelectron spectroscopy of oxidized pyrrhotite surfaces: I. Exposure to aqueous solutions [J]. Appl Surf Sci, 1985, 20: 472−480.

[18] ALMEIDA C M V B, GIANNETTI B F. The electrochemical behavior of pyrite-pyrrhotite mixtures [J]. Journal of Electroanalytical Chemistry, 2003, 553: 27−34.

[19] ZHOU Hong-bo, ZENG Wei-ming, QIU Guan-zhou. Bioleaching of chalcopyrite concentrate by amoderately thermophilic culture in a stirred tank reactor [J]. Bioresource Technology, 2009, 100: 515−520.

[20] BIEGLER T, HORNE M D. The electrochemistry of surface oxidation of chalcopyrite [J]. Journal of the Electrochemical Society, 1985, 132(6): 1363−1369

[21] NAVA J L, OROPEZA M T, GONZALEZ I. Electrochemical characterisation of sulfur species formed during anodic dissolution of galena concentrate in perchlorate medium at pH 0 [J]. Electrochimica Acta, 2002, 47(10): 1513−1525.

[22] EGHBALNIA M, DIXON D G. Electrochemical study of leached chalcopyrite using solid paraffin-based carbon paste electrodes [J]. Hydrometallurgy, 2011, 110(1/2/3/4): 1−12.

[23] ZENG Wei-ming, QIU Guan-zhou, ZHOU Hong-bo, CHEN Miao. Electrochemical behaviour of massive chalcopyrite electrodes bioleached by moderately thermophilic microorganisms at 48 °C [J]. Hydrometallurgy, 2011, 105(3/4): 259−263.

(Edited by YANG Hua)